HIV Protease Inhibitor Nelfinavir Inhibits Growth of Human Melanoma Cells by Induction of Cell Cycle Arrest

Wei Jiang,[1] Peter J. Mikochik,[2] Jin H. Ra,[1] Hanqin Lei,[1] Keith T. Flaherty,[3] Jeffrey D. Winkler,[2] and Francis R. Spitz[1]

[1]Division of Endocrine and Oncologic Surgery, Department of Surgery, University of Pennsylvania Medical Center; [2]Department of Chemistry and [3]Abramson Cancer Center, University of Pennsylvania, Philadelphia, Pennsylvania

Abstract

HIV protease inhibitors (HIV PI) are a class of antiretroviral drugs that are designed to target the viral protease. Unexpectedly, this class of drugs is also reported to have antitumor activity. In this study, we have evaluated the *in vitro* activity of nelfinavir, a HIV PI, against human melanoma cells. Nelfinavir inhibits the growth of melanoma cell lines at low micromolar concentrations that are clinically attainable. Nelfinavir promotes apoptosis and arrests cell cycle at G_1 phase. Cell cycle arrest is attributed to inhibition of cyclin-dependent kinase 2 (CDK2) and concomitant dephosphorylation of retinoblastoma tumor suppressor. We further show that nelfinavir inhibits CDK2 through proteasome-dependent degradation of Cdc25A phosphatase. Our results suggest that nelfinavir is a promising candidate chemotherapeutic agent for advanced melanoma, for which novel and effective therapies are urgently needed. [Cancer Res 2007;67(3):1221–7]

Introduction

Metastatic melanoma remains a serious clinical challenge. Currently, there is no proven effective therapy to improve survival of metastatic melanoma patients. Dacarbazine and related compound, temozolomide, remain the standard chemotherapy. However, for dacarbazine or temozolomide, the overall response rate is only 15% to 20%, with median response duration of about 4 to 6 months. Various combinations of chemotherapy, immunotherapy, and vaccine strategies have also failed to show survival advantages compared with single-agent therapies (1). New strategies are urgently needed to decrease morbidity and enhance survival of melanoma patients.

HIV protease inhibitors (HIV PI) are a class of small-molecule drugs that were rationally designed to target the viral aspartyl protease. Currently, there are nine Food and Drug Administration–approved HIV PIs, including commonly prescribed drugs ritonavir, saquinavir, indinavir, and nelfinavir. These drugs, given in combination with reverse transcriptase inhibitors, are the mainstays of the current therapeutic regimens for HIV-infected patients. In recent years, there have been increasing interests in evaluating HIV PIs as antineoplastic agents. Early support for this concept came from the observation that patients on highly active antiretroviral therapy had a reduced risk of developing HIV-associated malig-

nancies, such as Kaposi's sarcoma and non–Hodgkin's lymphoma. Highly active antiretroviral therapy had also led to regression of these tumors (2). Intuitively, such antitumor activity was attributed to suppression of HIV infection and reconstitution of immune functions. However, several recent studies support the notion that HIV PIs have direct antitumor activities that are independent of their antiviral activity. It was first reported that saquinavir, indinavir, and ritonavir enhanced the antiproliferative and differentiating activity of all-*trans*-retinoic acid for myelocytic leukemia cells (3). Sgadari et al. (4) reported that indinavir and saquinavir potently inhibited angiogenesis and induced regression of Kaposi's sarcoma–like lesions in nude mice. Subsequently, several HIV PIs have been shown to inhibit cell growth and/or induce apoptosis in various cancer cell types, including Kaposi's sarcoma (5), lymphoma, fibrosarcoma (6), multiple myeloma (7), prostate cancer (8, 9), and breast cancer (10). Currently, there are several prospective clinical trials under way in Italy that evaluate HIV PIs on HIV-associated cancers (Kaposi's sarcoma and non–Hodgkin's lymphoma) and non–HIV-associated cancers (Kaposi's sarcoma and non–small cell lung carcinoma; ref. 2). The results of those trials have not been reported.

Despite mounting evidence that supports HIV PIs as promising antineoplastic agents, enthusiasm for these drugs is limited by the lack of understanding of their antitumor mechanisms. Previous studies have pointed to multiple cellular signaling pathways as being perturbed by HIV PIs, which include proteasome, nuclear factor-κB, Akt, and signal transducers and activators of transcription 3 (6, 7, 10, 11). It is not clear what cellular molecules are directly targeted by HIV PIs or how HIV PIs affect the above-mentioned signaling pathways. Understanding the molecular mechanisms underlying antitumor activity of HIV PIs will be essential for further development of this class of agents.

In this study, we provide preclinical data for the use of HIV PI nelfinavir as a chemotherapeutic agent against melanoma. We show here that nelfinavir has excellent antitumor activity against human melanoma cells *in vitro*. Nelfinavir induces both G_1 cell cycle arrest and apoptosis in melanoma cell lines. Nelfinavir causes G_1 arrest by dramatically reducing the activity of cyclin-dependent kinase (CDK2) and thereby causing dephosphorylation of the retinoblastoma (Rb) tumor suppressor. Inhibition of CDK2 activity by nelfinavir treatment is mediated in part by proteasome-dependent degradation of Cdc25A phosphatase.

Materials and Methods

Cell culture. Human epidermal melanocytes HEMn-LP (Cascade Biologics, Portland, OR) were grown in Medium 254 supplemented with phorbol 12-myristate 13-acetate–free human melanocyte growth supplement (Cascade Biologics). All human melanoma cell lines, except A375, were grown in 2% melanoma medium [4 volumes of MCDB153 medium,

1 volume of Leibovitz's L-15 medium, supplemented with 2% fetal bovine serum (FBS), 5 μg/mL insulin, and 1.68 mmol/L CaCl$_2$]. A375 cells were grown in DMEM supplemented with 10% FBS and 2 mmol/L glutamine. All cells were maintained at 37°C in a 5% CO$_2$ incubator.

Chemicals and reagents. Nelfinavir mesylate tablets (Viracept) were purchased from the manufacturer Pfizer, Inc (New York, NY). Tablets were pulverized and suspended in a biphasic ethyl acetate (100 mL)/10% Na$_2$CO$_3$ aqueous solution (75 mL) mixture. The solution was stirred for 30 min, and organic phase was separated from the aqueous phase via separatory funnel. The aqueous layer was reextracted with ethyl acetate (2 × 50 mL). The organic phases were combined, rinsed with saturated NaCl solution, and desiccated over Na$_2$SO$_4$. The solvent was removed under reduced pressure to yield nelfinavir free base. The product was then suspended in methylene chloride (75 mL), and methanesulfonic acid (1.5 molar equivalents) was added dropwise over 5-min period. The solution was stirred for additional 20 min followed by solvent removal under reduced pressure. The solid was suspended in cold diethyl ether (30 mL) and filtered via a Buchner apparatus to yield pure nelfinavir mesylate. The purity of nelfinavir preparation was verified by nuclear magnetic resonance analysis. Purified nelfinavir was dissolved in ethanol to make 20 mmol/L stock solution that was used for all experiment in this study. MG-132 was purchased from EMD Biosciences (San Diego, CA). All other chemicals were purchased from Sigma-Aldrich (St. Louis, MO) unless noted otherwise. The antibodies used in this study are as follows: Cdc25A (Lab Vision, Fremont, CA), CDK2 (Santa Cruz Biotechnology, Santa Cruz, CA), cyclin E (Santa Cruz Biotechnology), actin (Santa Cruz Biotechnology), and myc (Invitrogen, Santa Cruz, CA). The following antibodies are from Cell Signaling (Danvers, CA): p21, p27, Rb, phosphorylated Rb Ser[608], Akt, phosphorylated Akt Ser[473], phosphorylated Chk2 Thr[68], and FLAG.

Cell counting analysis. Cells (1 × 10⁵) were seeded in 12-well plates. Nelfinavir was added to culture medium on the next day. After 24 or 48 h, adherent cells were trypsinized and resuspended in culture medium containing 0.2% trypan blue. The numbers of trypan blue–excluding cells were counted using a hemocytometer. Triplicate wells were counted for each condition. The data were presented as relative cell viability, in which untreated cells at a given time point were set as 100%.

Cell cycle analysis. Cells (5 × 10⁵) were seeded in 60-mm dishes 20 h before experiment. Cells were treated with 15 μmol/L nelfinavir or equivalent ethanol vehicle for 8, 16, and 24 h. Adherent cells were then trypsinized and resuspended in cold PBS with 1% FBS. Three volumes of cold 75% ethanol were added in a dropwise manner while vortexing. Cells were fixed for 24 h at 4°C, washed twice with cold PBS with 1% FBS, and resuspended in PBS with 1% FBS, 10 μg/mL propidium iodide, and 50 μg/mL RNase A. Final cell suspensions were incubated at 37°C for 30 min followed by flow cytometry analysis. Flow cytometry data was acquired using the Guava PCA system and analyzed using the Cell Cycle module of CytoSoft software (Guava Technologies, Hayward, CA). Data shown in this article are representative of two independent experiments.

Melanoma spheroid assay. The method was adapted from Smalley et al. (12). Briefly, 5,000 melanoma cells were seeded on top of 1.5% agarose in 96-well plate. After 72 h of incubation, melanoma spheroids were harvested by aspiration and embedded in collagen gels that contained 2 mg/mL rat tail type I collagen (BD Biosciences, Bedford, MA), Eagle's MEM, ʟ-glutamine, 2% FBS, and varying amounts of nelfinavir. Normal 2% melanoma medium containing proper amount of nelfinavir was added on top of solidified gel. After 72 h of incubation, spheroids were washed with PBS and stained with calcein-AM and ethidium bromide for 1 h. Images of representative spheroids were taken using an inverted fluorescent microscope.

Apoptosis assay. WM115 cells (5 × 10⁵) were seeded in 60-mm dishes. On the next day, cells were treated with either vehicle control (ethanol) or varying concentrations of nelfinavir. After 24 and 48 h, cells (both floating and adherent) were collected by trypsinization, washed once with 1 mL 1× Nexin buffer, and stained with Annexin V and 7-aminoactinomycin D (7-AAD) according to the manufacturer's protocol. Stained cells were immediately analyzed with the Guava PCA system using the Nexin module of CytoSoft software. Results shown are representative of two independent experiments.

CDK2 kinase activity assay. Cells (both untreated and nelfinavir treated) were washed twice with cold PBS, scraped off culture dishes, and collected by centrifugation. Cell pellets were snap frozen and stored at −80°C. Frozen cell pellets were resuspended in 5 volumes of kinase lysis buffer [50 mmol/L Tris (pH 8.0), 150 mmol/L NaCl, 2.5 mmol/L EGTA, 1 mmol/L EDTA, 1 mmol/L DTT, 0.1% Tween 20] supplemented with 1 mmol/L phenylmethylsulfonyl fluoride, 50 μmol/Lleupeptin, 17 μg/mL aprotinin, 1 mmol/L sodium vanadate, 10 mmol/L NaF, and 1× phosphatase inhibitor cocktail I and II (Sigma-Aldrich). Cell lysates were incubated on ice for 20 min with occasional vortexing and cleared by centrifugation at 13,000 rpm for 10 min. Cell lysates (each containing 200 μg total protein in 500 μL volume) were mixed with 30 μL protein A agarose beads (Invitrogen) and incubated with rocking for 30 min. Protein A beads were removed by centrifugation at 3,000 rpm for 3 min. Supernatants were mixed with 1 μg anti-CDK2 antibody (Santa Cruz Biotechnology) and incubated with rocking overnight. Protein A beads were then added to each sample and incubated for 2 h with rocking. Beads were washed twice with kinase lysis buffer and twice with kinase reaction buffer [50 mmol/L Tris (pH 7.5), 10 mmol/L MgCl$_2$, 1 mmol/L EGTA, 1 mmol/L DTT, 1 mmol/L sodium vanadate, and 10 mmol/L NaF]. After the final wash, beads were resuspended with 56.5 μL reaction mixture (kinase reaction buffer plus 2 μmol/L ATP, 100 ng/μL histone H1, and 0.1 μCi/μL [γ-³²P]ATP). Reactions were incubated at 30°C for 1 h and stopped by adding 10 μL 6× SDS sample buffer. Samples were resolved on a 10% SDS-PAGE gel and visualized by autoradiography. Similar results were obtained from two independent experiments.

Immunoblotting assay. Cells were lysed with NP40 lysis buffer [50 mmol/L Tris (pH 7.5), 150 mmol/L NaCl, 1 mmol/L EDTA, 1% NP40] supplemented with protease and phosphatase inhibitors. Whole-cell lysates were resolved on a 10% SDS-PAGE gel and transferred to polyvinylidene difluoride membrane blots. Blots were incubated with respective primary antibodies overnight. Horseradish peroxidase–conjugated secondary antibodies were used for chemiluminescence detection. Immunoblotting data in this article are representative of at least two independent experiments.

Results

Nelfinavir inhibits cell growth and promotes apoptosis in melanoma cell lines *in vitro*. We tested several HIV PIs for their effect on growth of melanoma cell line WM35. Tested drugs include nelfinavir, ritonavir, saquinavir, and indinavir. The four drugs showed very different activity against WM35 cells. Nelfinavir was the most active drug, with a IC$_{50}$ of ~5.5 μmol/L. Ritonavir was slightly less active than nelfinavir, whereas saquinavir and indinavir had essentially no activity at concentrations up to 20 μmol/L (Fig. 1*A*). Because nelfinavir showed the highest activity against melanoma cells, we focused our subsequent investigations on this drug.

The activity of nelfinavir against additional human melanoma and colon cancer cell lines was determined as summarized in Table 1. It is notable that the IC$_{50}$ of nelfinavir for most tested cell lines is between 5 and 12 μmol/L. This concentration is attainable in the plasma of human patients who take nelfinavir at standard dosage. Melanoma cell lines (WM35 and 1205LU) are more sensitive to nelfinavir than normal human melanocytes (HEMn-LP), suggesting that transformed cells may be preferentially susceptible to nelfinavir (Fig. 1*B*). It is also interesting to note that cell lines derived from metastatic melanoma (C8161, 1205LU, and NIH1286) are similarly susceptible to nelfinavir compared with cell lines derived from early-stage melanoma (WM35 and WM115; Table 1).

Anchorage-independent growth is a unique characteristic of transformed cells. We asked whether nelfinavir could block anchorage-independent growth of melanoma cells. WM115 cells that were seeded in soft agar gel formed large visible colonies within 2 weeks. When these cells were grown in the presence of
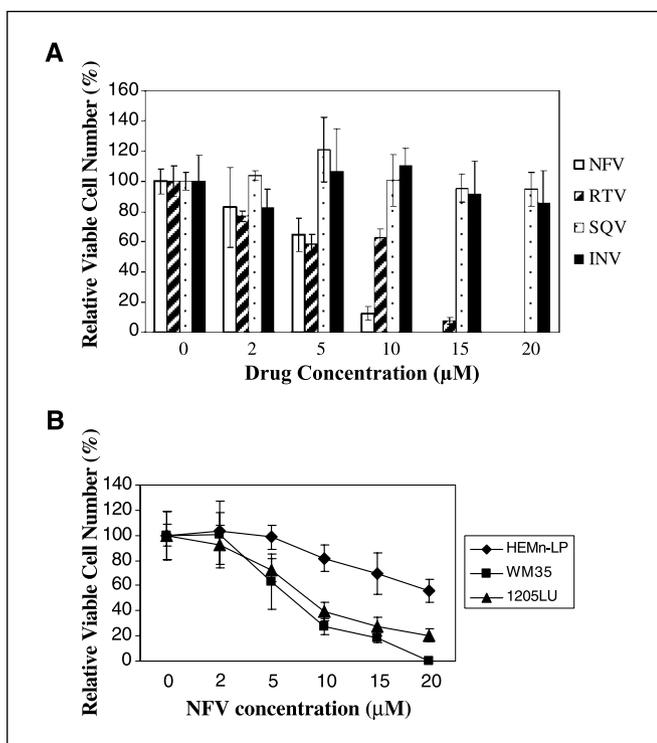
Figure 1. Nelfinavir inhibits growth of melanoma cells *in vitro*. *A,* WM35 melanoma cells were cultured in the presence of varying concentrations of HIV PIs for 48 h. *NFV,* nelfinavir; *RTV,* ritonavir; *SQV,* saquinavir; *INV,* indinavir. *B,* melanoma cells (WM35 and 1205LU) and normal melanocytes (HEMn-LP) were cultured in the presence of varying concentrations of nelfinavir for 24 h. Numbers of viable cells were counted using trypan blue staining. Data are presented as percentage of relative cell viability, where untreated cells were set as 100%. Cell counting was done in triplicate. *Bars,* SD.

5 µmol/L nelfinavir, only very small colonies appeared. Growth in soft agar gel was almost completely blocked by 10 µmol/L nelfinavir (Fig. 2*A*).

A novel melanoma spheroid culture model has been developed recently that mimics *in vivo* tumor microenvironment (12). We tested the ability of nelfinavir to block growth of aggressive melanoma cells in this model. Consistent with previous results, spheroids formed by C8161 and 1205LU cells grew and invaded rapidly into embedding collagen matrix. Nelfinavir inhibited growth and invasion of both cell lines in a dose-dependent manner (Fig. 2*B*). At 20 µmol/L, nelfinavir almost completely blocked melanoma cell invasion into collagen matrix and greatly reduced cell viability.

Microscopic observations revealed significant cell death, in addition to growth arrest, after nelfinavir treatment (data not shown). We therefore asked whether nelfinavir could also promote apoptotic cell death. WM115 cells were treated with varying doses of nelfinavir for 24 or 48 h after which apoptotic cells were analyzed by Annexin V staining. Nelfinavir treatment increased the population of both Annexin V–positive/7-AAD–negative cells (early apoptotic) and Annexin V–positive/7-AAD–positive (late apoptotic/dead) cells in a dose-dependent manner (Fig. 2*C*).

Nelfinavir induces G_1 cell cycle arrest in melanoma cells through inhibition of CDK2. Cell cycle arrest is an important antitumor mechanism of radiotherapy/chemotherapy. We asked whether the antitumor activity of nelfinavir involved cell cycle arrest. Nelfinavir treatment caused a marked G_1 arrest in WM35

cells as indicated by increased percentage of cells at G_1 phase and decreased percentage of cells at S and G_2-M phase. The G_1 arrest was evident after nelfinavir treatment as short as 8 h and reached maximal extent by 24 h (Fig. 2*D*). Similar results were observed in WM115 and A375 cells (data not shown).

CDKs play key roles in regulating cell cycle progression in eukaryotic cells. Among mammalian CDKs, CDK2 is considered a master switch that controls G_1-S cell cycle progression. The best-studied substrate of CDK2 is the Rb protein. CDK2 phosphorylates Rb at multiple serine and threonine residues, which causes dissociation of Rb from E2F family of transcription factors. Free E2F then activates transcription of target genes that are required for DNA synthesis (13). To elucidate the mechanism of nelfinavir-induced G_1 arrest, we investigated the effect of nelfinavir on the CDK2-Rb pathway. Nelfinavir treatment caused a sharp decline in CDK2 activity within 24 h (Fig. 3*A*). The kinetics of CDK2 inactivation is consistent with that of nelfinavir-induced G_1 arrest. CDK2 inactivation was accompanied by decreased phosphorylation of Rb at Ser^{608} (Fig. 3*B*). Total Rb protein level remained unchanged after nelfinavir treatment. These data suggest that inactivation of CDK2-Rb axis is an important mechanism of nelfinavir-induced G_1 cell cycle arrest.
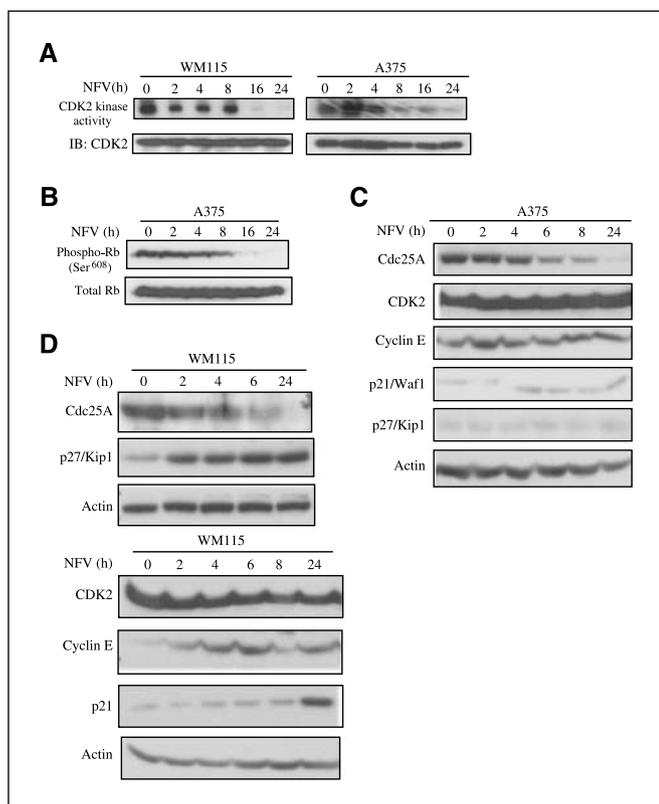
Activity of CDK2 is regulated at multiple levels: protein level of CDK2 and its binding partner cyclin E, binding of CDK inhibitors p21 or p27 to cyclin E-CDK2 complex, and post-translational modification of CDK2. Phosphorylation of CDK2 at Thr^{14} and Tyr^{15} by Wee1 kinase inhibits CDK2 activity. Phosphorylated groups at Thr^{14} and Tyr^{15} can be removed by Cdc25A phosphatase, resulting in CDK2 activation. To elucidate how nelfinavir inhibits CDK2 activity, we examined the level of several key CDK2 regulators. Nelfinavir treatment did not significantly change the level of CDK2 itself or cyclin E in either WM115 or A375 cells. CDK inhibitors p21 and p27 were strongly induced by nelfinavir treatment in WM115 cells but not in A375 cells (Fig. 3*C* and *D*). The induction of p27 in WM115 cells occurred rather early (2 h), whereas p21 induction was only detected after 24 h. In both WM115 and A375 cells, nelfinavir treatment induced a sharp decrease in the level of Cdc25A phosphatase. Decrease in Cdc25A level either preceded (in WM115 cell) or coincided (in A375 cell) with CDK2 inactivation, suggesting that the decrease in Cdc25A is likely the primary factor that causes CDK2 inactivation and cell cycle arrest (Fig. 3*C* and *D*).

Table 1. IC$_{50}$ of nelfinavir for colon cancer and melanoma cell lines

Colon cancer cell lines	IC$_{50}$ (µmol/L)	Melanoma cell lines	IC$_{50}$ (µmol/L)
Colo205	6.6	1205LU	4.0
HCT-116	10.5	A375	11.0
HT-29	8.6	C8161	6.5
KM12L4	9.0	NIH1286	5.0
SW480	30.0	WM35	5.5
SW620	15.0	WM115	6.7

NOTE: Cells were treated with varying amounts of nelfinavir for 48 h. Viable cells were counted using trypan blue staining. Cell counting was done in triplicate. IC$_{50}$ was estimated by curve fitting.

Proteasomal degradation plays an important role in the regulation of Cdc25A. In DNA damage-induced G_1 checkpoint, DNA damage activates the ATM/ATR-Chk1/Chk2 signaling cascade (14). Activated Chk1 or Chk2 phosphorylates Cdc25A at several serine residues (most notably Ser[76] and Ser[124]), which promotes association of Cdc25A with E3 ubiquitin ligase, such as β-TrCP, and subsequent polyubiquitination/degradation (15–17). We decided to investigate whether down-regulation of Cdc25A by nelfinavir was

Figure 2. Activity of nelfinavir in various *in vitro* assays. *A,* nelfinavir inhibits anchorage-independent growth of melanoma cells. WM115 cells were seeded in soft agar plates that were overlaid with medium containing varying amounts of nelfinavir. Cells were cultured for 14 d and observed with inverted phase-contrast microscope. *B,* nelfinavir inhibits growth of melanoma spheroids in collagen gel. C8161 and 1205LU cells were grown for 3 d as spheroids embedded in type I collagen gel. Cells were stained with calcein-AM and ethidium bromide and observed with inverted fluorescent microscope. Live cells were stained *green* (calcein-AM) and dead cells were stained *red* (ethidium bromide). *C,* nelfinavir promotes apoptotic cell death of melanoma cells. WM115 cells were incubated with varying amounts of nelfinavir or vehicle control [ethanol (*EtOH*)] for 48 h. Both adherent and floating cells were then harvested, pooled, and stained with Annexin V-phycoerythrin and 7-AAD. Stained cells were analyzed by flow cytometry. *Top,* representative flow cytometry dot plot; *bottom,* bar graph showing percentage of early apoptotic cells (*Annexin V[+]/7-AAD[−]*) and late apoptotic/dead cells (*Annexin V[+]/7-AAD[+]*). *D,* nelfinavir induces cell cycle arrest at G_1 phase. WM35 cells were incubated with 15 μmol/L nelfinavir or vehicle control (ethanol) for varying times. Adherent cells were harvested by trypsinization. After ethanol fixation, cells were stained with propidium iodide and analyzed by flow cytometry. Percentage of cell in each phase is indicated. Data are representative of two independent experiments. Similar results were observed with WM115 and A375 cells (data not shown).

Figure 3. Nelfinavir induces G₁ arrest through inhibition of CDK2 activity. *A,* WM115 and A375 cells were treated with 15 μmol/L nelfinavir for varying times. Cell lysates were immunoprecipitated with anti-CDK2 antibody. Precipitates were assayed for kinase activity using histone H1 substrate. *B,* A375 cells were treated as in (*A*). Cell lysates were subjected to immunoblotting to detect Ser^{608}-phosphorylated Rb or total Rb. *C* and *D,* immunoblotting analysis for regulators of CDK2. A375 (*C*) and WM115 (*D*) cells were treated with 15 μmol/L nelfinavir for varying times. Cell lysates were subjected to immunoblotting analysis using indicated antibodies.

also mediated by this pathway. First, we asked whether proteasome inhibitor would block nelfinavir-induced Cdc25A down-regulation. WM115 cells were pretreated with either DMSO (vehicle control) or 5 μmol/L MG-132 (a proteasome inhibitor) and then treated with 15 μmol/L nelfinavir for varying times. Immunoblotting showed that MG-132 completely abolished nelfinavir-induced decrease of Cdc25A level, suggesting that the down-regulation of Cdc25A by nelfinavir is indeed mediated by proteasomal degradation (Fig. 4*A*).

Next, we examined Thr^{68} phosphorylation level of Chk2 after nelfinavir treatment. Thr^{68} phosphorylation is a prerequisite for activation of Chk2. Nelfinavir treatment significantly increased Thr^{68} phosphorylation of Chk2 as revealed by immunoblotting (Fig. 4*B*).

Finally, we examined the effect of mutations in Cdc25A degradation motifs on nelfinavir-induced degradation. Two degradation motifs in Cdc25A have been characterized, the $D_{81}S_{82}G_{83}$ motif and the $K_{141}E_{142}N_{143}$ motif, which are required for β-TrCP–mediated or APC/C-Cdh1–mediated ubiquitination, respectively (15, 16). WM115 cells were transfected with either wild-type or mutant Cdc25A cDNA that harbors mutation in either the DSG motif (S76A/S82A/S88A, SA mutant) or the KEN motif (K141A/E142A/N143A, K2M mutant). Ectopically expressed Cdc25A was detected by immunoblotting using epitope-specific antibodies. As shown in Fig. 4*C*, wild-type Cdc25A was degraded efficiently after

nelfinavir treatment, whereas both mutants remained stable after nelfinavir treatment.

Taken together, these data showed that nelfinavir treatment promoted proteasomal degradation of Cdc25A that was dependent on both the DSG and KEN degradation motifs. In addition, nelfinavir activated Thr^{68} phosphorylation of Chk2, suggesting that activated ATM-Chk2 signaling pathway may be involved in nelfinavir-induced degradation of Cdc25A.

Inhibition of Akt signaling is an unlikely mechanism. Several studies suggested that inhibition of phosphatidylinositol 3-kinase/Akt signaling was an important antitumor mechanism of HIV PIs. Srirangam et al. (10) showed that 24 h of ritonavir treatment decreased Ser^{473} phosphorylation of Akt in breast cancer cell lines. Gupta et al. (11) showed that treatment of cells harboring activated Akt allele with subcytotoxic doses of HIV PIs led to decreased Akt phosphorylation after prolonged incubation. In both cases, the mechanisms by which HIV PIs inhibit Akt signaling were unknown.

We asked whether nelfinavir also led to inhibition of Akt signaling in melanoma cells. WM35, WM115, and A375 cells were incubated with nelfinavir for varying times. Cell lysates were
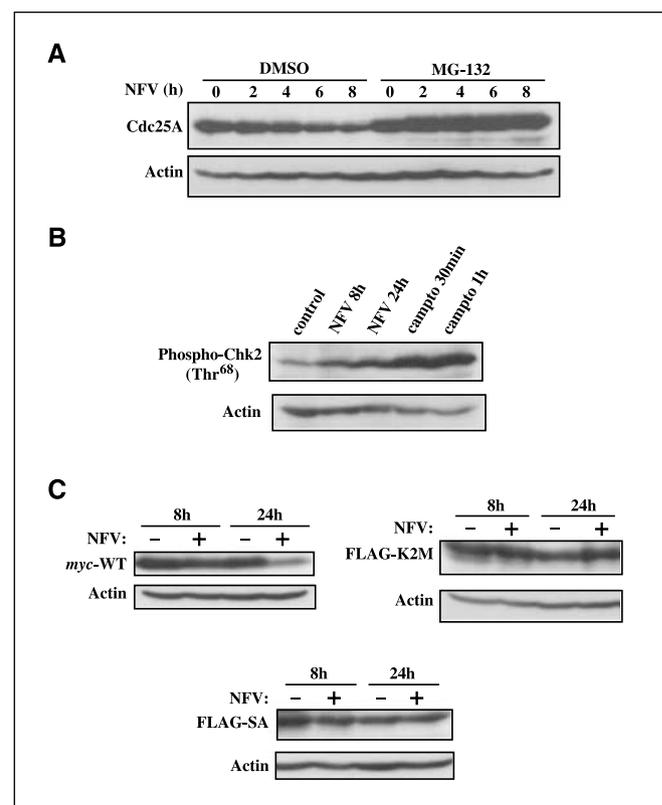
Figure 4. Nelfinavir induces proteasome-dependent degradation of Cdc25A. *A,* WM115 cells were pretreated with either DMSO or 5 μmol/L MG-132 for 30 min. Nelfinavir was then added to culture medium to make 15 μmol/L concentration. Cells were harvested after varying incubation times. Cell lysates were subjected to immunoblotting for Cdc25A. *B,* WM115 cells were treated with 15 μmol/L nelfinavir or 20 μmol/L camptothecin (*campto*) for indicated time. Lysates from untreated and treated cells were immunoblotted for Thr^{68}-phosphorylated Chk2. Camptothecin-treated cells serve as positive control for Chk2 phosphorylation. Actin was used as loading control. *C,* WM115 cells were transfected with various Cdc25A expression plasmids: *myc*-tagged wild-type, FLAG-tagged K2M mutant, or FLAG-tagged SA mutant. Forty-eight hours after transfection, cells were treated with either ethanol or nelfinavir (15 μmol/L) for indicated time. Ectopically expressed Cdc25A was detected by immunoblotting using *myc* or FLAG antibody.
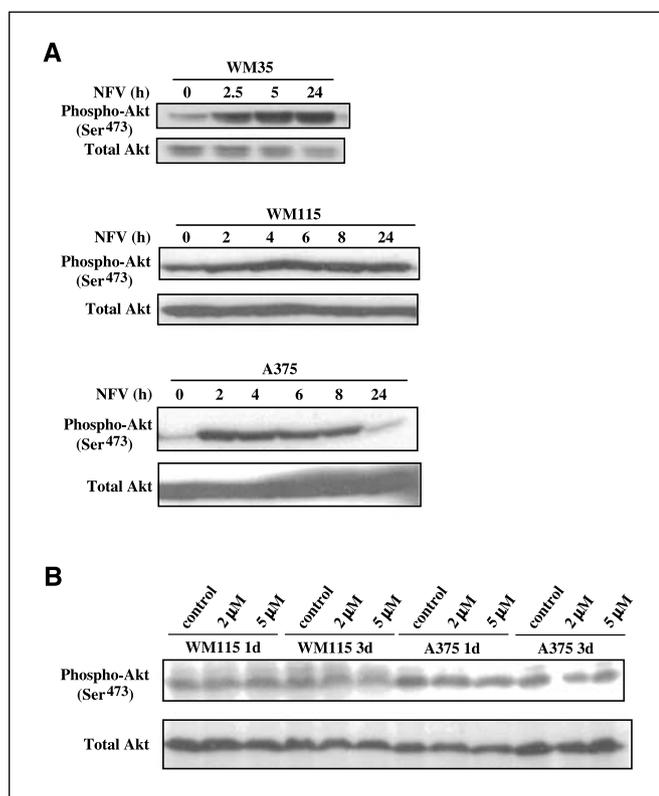
Figure 5. Inhibition of Akt signaling is an unlikely antitumor mechanism of nelfinavir for melanoma cells. *A,* melanoma cells (*WM35*, *WM115*, and *A375*) were treated with nelfinavir for indicated time. Nelfinavir dosage is as follows: 10 μmol/L for WM35 and 15 μmol/L for WM115 and A375. Ser^{473}-phosphorylated Akt and total Akt were detected by immunoblotting. *B,* WM115 and A375 cells were treated with low dose of nelfinavir (2 and 5 μmol/L) for 1 or 3 d. Cell lysates were immunoblotted for phosphorylated Ser^{473} and total Akt.

subjected to immunoblotting analysis to detect Ser^{473} phosphorylation of Akt. In all three cell lines, nelfinavir treatment significantly increased Ser^{473} phosphorylation of Akt, whereas total Akt protein level was not affected (Fig. 5*A*). Akt phosphorylation was elevated rapidly (within 2–2.5 h) in all three cell lines. Interestingly, elevated Akt phosphorylation was sustained for up to 24 h in WM35 and WM115 cells but transient in A375 cells. Subcytotoxic dosage of nelfinavir (2–5 μmol/L) had no significant effect on Akt phosphorylation even after 72 h of incubation (Fig. 5*B*). We conclude that nelfinavir does not inhibit Akt signaling pathway in melanoma cells. Therefore, inhibition of Akt signaling is unlikely to be a major antitumor mechanism of nelfinavir in melanoma cells.

Discussion

In this study, we present preclinical data on the antitumor activity of HIV PI nelfinavir in human melanoma cell lines. Nelfinavir inhibits growth of most cancer cell lines in our test panel with IC$_{50}$ between 5 and 12 μmol/L. Importantly, this is a concentration that is comparable with peak plasma concentration in patients and healthy volunteers who take nelfinavir at recommended dose. In a phase I/II trial, nelfinavir was administered to HIV-infected patients at a dosage of 500 or 750 mg thrice daily. Peak plasma concentration of nelfinavir in these patients was in the range of 3 to 4 μg/mL (4.5–6.0 μmol/L; ref. 18). In another

study, healthy volunteers were given once-daily combination of 2,000 mg nelfinavir and low-dose (200 or 400 mg) ritonavir. Peak plasma nelfinavir concentration of 5.1 to 7.2 μg/mL (7.7–10.8 μmol/L) was detected (19). Furthermore, because serious dose-limiting toxicity has not been observed for nelfinavir, it is possible to administer nelfinavir at an even higher dose and in combination with ritonavir, which is known to increase drug exposure of nelfinavir (20), to achieve therapeutic drug level that exceeds *in vitro* IC$_{50}$ in human patients. Another interesting finding from this study is that cell lines derived from metastatic melanoma, which are usually more resistant to conventional cytotoxic agents, are similarly susceptible to nelfinavir treatment compared with cell lines derived from early-stage melanoma. This suggests that nelfinavir may act on cancer cells with a mechanism distinct from those of conventional chemotherapeutics.

Conventional cell culture on plastic dishes is often regarded as an inadequate model for testing cancer therapeutics partly because it does not reflect the interaction between cancer cells with its stromal matrix. A novel melanoma spheroid model has been developed recently in which melanoma cells were grown as three-dimensional spheroids and then embedded in type I collagen gel to mimic the *in vivo* tumor microenvironment (12). This model is expected to give better prediction of *in vivo* response of novel cancer therapeutics. Nelfinavir shows excellent activity in this assay, blocking both growth and invasion of metastatic melanoma cells. The effective dosage of nelfinavir in this assay (>10 μmol/L) is higher than that for two-dimensional culture, which probably reflects the prosurvival property of collagen matrix.

We further investigated the effects of nelfinavir on melanoma cells in additional *in vitro* assays. Nelfinavir inhibits anchorage-independent growth, promotes apoptotic cell death, and induces G$_1$ cell cycle arrest. It is likely that apoptosis and cell cycle arrest both contribute to the antitumor activity of nelfinavir. We investigated the molecular mechanism of nelfinavir-induced G$_1$ cell cycle arrest in further detail. Nelfinavir treatment induces dramatic decrease in the activity of CDK2, the master kinase that controls G$_1$-S progression in mammalian cells. Inhibition of CDK2 activity is not due to decreased protein level of CDK2 or its cyclin partner cyclin E. Although nelfinavir does lead to accumulation of CDK inhibitors p21 and p27 in WM115 cell line, this effect is not observed in another cell line, A375. A more likely mechanism of CDK2 inhibition is decreased level of Cdc25A phosphatase, which is observed in both WM115 and A375 cells.

Cdc25A is an essential component of the ATR/ATM-Chk1/Chk2-Cdc25A signaling cascade that controls G$_1$-S checkpoint. In response to DNA damage caused by ionizing irradiation or replication block, ATM/ATR kinases are activated that in turn phosphorylate and activate Chk1/Chk2 kinases. Chk1/Chk2 kinases directly phosphorylate Cdc25A primarily on Ser^{76} or Ser^{124} depending on the specific stimuli. Phosphorylation by Chk1/Chk2 promotes ubiquitination of Cdc25A by E3 ubiquitin ligases (such as β-TrCP) and rapid proteasomal degradation. In this study, we present evidence, which suggests that nelfinavir induces Cdc25A degradation via a similar mechanism. First, nelfinavir-induced Cdc25A degradation is dependent on proteasome activity. Second, nelfinavir induces activation of Chk2 kinase. Third, degradation of Cdc25A after nelfinavir treatment is dependent on two degradation motifs in Cdc25A protein: the KEN box and the DSG motif. Mutant Cdc25A proteins that harbor point mutations in either motif cannot be degraded after nelfinavir treatment.

It was previously reported that ritonavir could inhibit the chymotrypsin-like activity of the 20 S proteasome (21). This has been cited as an antitumor mechanism of ritonavir (6). However, it seems to us that direct inhibition of proteasome by nelfinavir is probably not the primary antitumor mechanism due to the following reasons. First, in the original report (21), nelfinavir did not inhibit the chymotrypsin-like activity of 20 S proteasome even at a concentration of 100 μmol/L (which far exceeds IC_{50} of nelfinavir for any melanoma cell lines tested). Second, our data show that nelfinavir promotes proteasomal degradation of Cdc25A, which is incompatible with the proteasome inhibition hypothesis. Third, although we did observe accumulation of p21 and p27 after nelfinavir treatment in WM115 cell line (which would agree with the proteasome inhibition hypothesis), such effect was not observed in A375 cells, suggesting that accumulation of CDK inhibitors may not be a universal phenomenon.

Other investigators showed that HIV PIs (including nelfinavir) inhibit Akt signaling in tumor cell lines (10, 11). We did not observe inhibition of Akt signaling by nelfinavir in melanoma cells. Instead, we observed rapid elevation of Akt phosphorylation that indicated active Akt signaling. The reason for this apparent discrepancy is unknown. It is paradoxical that nelfinavir treatment leads to Akt activation in melanoma cells because Akt signaling is generally linked with cell proliferation and survival. However, our data show that nelfinavir induces cell cycle arrest and apoptosis in melanoma cells despite activated Akt signaling. We speculate that activation of Akt signaling may not be the direct result of nelfinavir action but rather reflects cellular responses to stress condition imposed by nelfinavir, a scenario analogous to Akt activation in response to glucose deprivation (22).

The molecular target(s) of nelfinavir (or HIV PIs in general) in cancer cells remains unknown. It is even uncertain whether different PIs share the same target or not. It was recently proposed that heat shock protein 90 (Hsp90) might be a target for ritonavir (10). Ritonavir binds Hsp90 with a K_d of 7.8 μmol/L and partially inhibits its chaperone activity. The relevance of Hsp90 to nelfinavir is not clear. The identification of the nelfinavir targets will be essential for the understanding of its antitumor mechanism. We are currently pursuing in this direction using biochemical and proteomic approaches.

Several features of nelfinavir make it an excellent chemotherapeutic candidate. The drug is very safe, which may be administered daily over many months or years. Unlike conventional chemotherapies, there are few hematologic, gastrointestinal, or neurologic side effects associated with nelfinavir. The drug has excellent bioavailability and well-characterized pharmacokinetic and pharmacodynamic properties. These features suggest that *in vitro* antitumor activity of nelfinavir is likely to be translatable into antitumor activity in animal models and even in clinical trials.

In summary, nelfinavir shows excellent *in vitro* activity against human melanoma cell lines. Nelfinavir inhibits cell growth by arresting cells at G_1 phase, which is mediated by proteasomal degradation of Cdc25A and concomitant inactivation of CDK2. Although the direct target(s) of nelfinavir remains unknown, our data argue that nelfinavir is a promising chemotherapeutic drug with potentially novel antitumor mechanisms. Further preclinical investigation in animal models and, potentially, clinical trial with advanced melanoma patients is warranted.

Acknowledgments

References

1. Tsao H, Atkins MB, Sober AJ. Management of cutaneous melanoma. N Engl J Med 2004;351:998–1012.
2. Monini P, Sgadari C, Toschi E, Barillari G, Ensoli B. Antitumour effects of antiretroviral therapy. Nat Rev Cancer 2004;4:861–75.
3. Ikezoe T, Daar ES, Hisatake J, Taguchi H, Koeffler HP. HIV-1 protease inhibitors decrease proliferation and induce differentiation of human myelocytic leukemia cells. Blood 2000;96:3553–9.
4. Sgadari C, Barillari G, Toschi E, et al. HIV protease inhibitors are potent anti-angiogenic molecules and promote regression of Kaposi sarcoma. Nat Med 2002;8:225–32.
5. Pati S, Pelser CB, Dufraine J, Bryant JL, Reitz MS, Jr., Weichold FF. Antitumorigenic effects of HIV protease inhibitor ritonavir: inhibition of Kaposi sarcoma. Blood 2002;99:3771–9.
6. Gaedicke S, Firat-Geier E, Constantiniu O, et al. Antitumor effect of the human immunodeficiency virus protease inhibitor ritonavir: induction of tumor-cell apoptosis associated with perturbation of proteasomal proteolysis. Cancer Res 2002;62:6901–8.
7. Ikezoe T, Saito T, Bandobashi K, Yang Y, Koeffler HP, Taguchi H. HIV-1 protease inhibitor induces growth arrest and apoptosis of human multiple myeloma cells via inactivation of signal transducer and activator of transcription 3 and extracellular signal-regulated kinase 1/2. Mol Cancer Ther 2004;3:473–9.
8. Ikezoe T, Hisatake Y, Takeuchi T, et al. HIV-1 protease inhibitor, ritonavir: a potent inhibitor of CYP3A4, enhanced the anticancer effects of docetaxel in androgen-independent prostate cancer cells *in vitro* and *in vivo*. Cancer Res 2004;64:7426–31.
9. Yang Y, Ikezoe T, Takeuchi T, et al. HIV-1 protease inhibitor induces growth arrest and apoptosis of human prostate cancer LNCaP cells *in vitro* and *in vivo* in conjunction with blockade of androgen receptor STAT3 and AKT signaling. Cancer Sci 2005;96:425–33.
10. Srirangam A, Mitra R, Wang M, et al. Effects of HIV protease inhibitor ritonavir on Akt-regulated cell proliferation in breast cancer. Clin Cancer Res 2006;12:1883–96.
11. Gupta AK, Cerniglia GJ, Mick R, McKenna WG, Muschel RJ. HIV protease inhibitors block Akt signaling and radiosensitize tumor cells both *in vitro* and *in vivo*. Cancer Res 2005;65:8256–65.
12. Smalley KS, Haass NK, Brafford PA, Lioni M, Flaherty KT, Herlyn M. Multiple signaling pathways must be targeted to overcome drug resistance in cell lines derived from melanoma metastases. Mol Cancer Ther 2006;5:1136–44.
13. Sherr CJ. The Pezcoller lecture: cancer cell cycles revisited. Cancer Res 2000;60:3689–95.
14. Sancar A, Lindsey-Boltz LA, Unsal-Kacmaz K, Linn S. Molecular mechanisms of mammalian DNA repair and the DNA damage checkpoints. Annu Rev Biochem 2004;73:39–85.
15. Busino L, Donzelli M, Chiesa M, et al. Degradation of Cdc25A by β-TrCP during S phase and in response to DNA damage. Nature 2003;426:87–91.
16. Donzelli M, Squatrito M, Ganoth D, Hershko A, Pagano M, Draetta GF. Dual mode of degradation of Cdc25 A phosphatase. EMBO J 2002;21:4875–84.
17. Mailand N, Falck J, Lukas C, et al. Rapid destruction of human Cdc25A in response to DNA damage. Science 2000;288:1425–9.
18. Markowitz M, Conant M, Hurley A, et al. A preliminary evaluation of nelfinavir mesylate, an inhibitor of human immunodeficiency virus (HIV)-1 protease, to treat HIV infection. J Infect Dis 1998;177:1533–40.
19. Aarnoutse RE, Droste JA, van Oosterhout JJ, et al. Pharmacokinetics, food intake requirements, and tolerability of once-daily combinations of nelfinavir and low-dose ritonavir in healthy volunteers. Br J Clin Pharmacol 2003;55:115–25.
20. Kempf DJ, Marsh KC, Kumar G, et al. Pharmacokinetic enhancement of inhibitors of the human immunodeficiency virus protease by coadministration with ritonavir. Antimicrob Agents Chemother 1997;41:654–60.
21. Andre P, Groettrup M, Klenerman P, et al. An inhibitor of HIV-1 protease modulates proteasome activity, antigen presentation, and T cell responses. Proc Natl Acad Sci U S A 1998;95:13120–4.
22. Awale S, Lu J, Kalauni SK, et al. Identification of arctigenin as an antitumor agent having the ability to eliminate the tolerance of cancer cells to nutrient starvation. Cancer Res 2006;66:1751–7.

HIV Protease Inhibitor Nelfinavir Inhibits Growth of Human Melanoma Cells by Induction of Cell Cycle Arrest

Wei Jiang, Peter J. Mikochik, Jin H. Ra, et al.

Updated version	Access the most recent version of this article at: http://cancerres.aacrjournals.org/content/67/3/1221

Cited articles	This article cites 22 articles, 14 of which you can access for free at: http://cancerres.aacrjournals.org/content/67/3/1221.full#ref-list-1
Citing articles	This article has been cited by 8 HighWire-hosted articles. Access the articles at: http://cancerres.aacrjournals.org/content/67/3/1221.full#related-urls

E-mail alerts	Sign up to receive free email-alerts related to this article or journal.
Reprints and Subscriptions	To order reprints of this article or to subscribe to the journal, contact the AACR Publications Department at pubs@aacr.org.
Permissions	To request permission to re-use all or part of this article, use this link http://cancerres.aacrjournals.org/content/67/3/1221. Click on "Request Permissions" which will take you to the Copyright Clearance Center's (CCC) Rightslink site.